

# Application of Soft Computing in the Design and Optimization of Tuned Liquid Column–Gas Damper for Use in Offshore Wind Turbines

Reza Dezvareh<sup>1\*</sup>

<sup>1\*</sup> Assistant Professor, Faculty of Civil Engineering, Babol Noshirvani University of Technology, Iran;  
[rdezvareh@nit.ac.ir](mailto:rdezvareh@nit.ac.ir)

## ARTICLE INFO

### Article History:

Received: 15 Feb. 2019

Accepted: 18 Mar. 2019

### Keywords:

offshore wind turbine  
tuned liquid column gas damper  
soft computing  
neural network  
Simulink model

## ABSTRACT

Tuned liquid column gas damper is a new type of energy absorber that can mitigate the vibrations of structures if their frequency and mass parameters are well tuned. Since this damper has recently been introduced and its behaviour in certain structures such as offshore oil platforms and wind turbines has already been tested, a suitable and accurate method is required to identify these optimal parameters. Therefore, considering the complexity of loads exerted on wind turbines in seas (wave and wind loads), in present study attempts are made to use a new artificial neural network approach to obtain optimal tuned liquid column–gas damper (TLCGD) parameters for mitigation of wind turbine vibrations. First fixed offshore wind turbines at various depths are designed in the MATLAB coding environment. After obtaining the stiffness, damping and mass matrices of the structures, the program enters the Simulink, and the wind turbine structure along with the TLCGD is exposed to different wave-wind load combinations within reasonable range of damper parameters. The neural network training is launched based on available statistical data of the offshore wind turbine with different heights as well as different frequency and mass ratios of the damper. According to this method, the percentage of errors found in the neural network outputs was negligible compared to the actual results obtained from the analysis in Simulink (even for inputs that stood outside the training range of the neural network). The mean error percentage, the standard deviation and the effective value of the neural network with actual values are below 10% for all three types of the structure. Finally, the method presented in this study can be used to obtain optimal parameters of the TLCGD for all kinds of offshore wind turbines at different depths of the sea, which leads to the optimal design of this damper to reduce the vibrations of wind turbines under wave and wind load pressures.

## 1. Introduction

Wind energy provides an environmentally friendly option. It can also provide sustainable development security when fossil fuels are reduced [1]. Nowadays, offshore wind turbine is one of the sources of wind energy in the world. Offshore wind turbines (OWTs) are one of the structures continuously under dynamic loads during their lifetime. It is also important to locate these turbines in the wind farm and calculate the optimum locations [2]. By installing the wind turbines in the sea, new issues arise when installing these structures on land, which are due to additional loads of the sea environment and special features of the design of this structure [3]. The vibration control devices have been invented and used to reduce the vibrations caused by wind, earthquake, and any other

dynamic load in a variety of structures. The tuned dampers, including TMD, TLCD, and TLCGD are one of the vibration reduction tools that are used passively. These dampers are of inactive (passive) type and their parameters are designed once according to the structure's characteristics, which remain constant throughout the exploitation time [4]. Moreover, recently semi-active damper (SALCGD) also assessed [5]. In other words, in addition to being permanently induced by vibrations and stimulations due to the wind loads, the loads resulting from the sea environment such as the wave load, sea flows, etc. are applied to the wind turbines. This led Lackner and Rotea (2011) [6] to study the inactive control of the vibrations of the offshore wind turbines. Lackner and Rotea (2011) [7] also examined the control of the

floating wind turbines vibrations. Later in 2011, Stewart and Lackner studied the effect of dynamic stimuli on the active control of the offshore wind turbines [8]. These studies have examined a variety of tuned dampers, including the tuned mass damper (TMD), the tuned liquid dampers (TLD), the tuned liquid column dampers (TLCD) and the active mass dampers (AMD) for two types of single-pile and floating wind turbines. Since, among the marine conditions, the load caused by the wave have a higher-lasting effect on the marine structures, the offshore wind turbines were controlled under the simultaneous stimulations of wave and wind in the latest research by the TLCD damper and its vibrations decreased [9]. Then, the effect of this damper on the reduction of forces caused by the earthquake was evaluated in the offshore wind turbine with the template support platform [10]. However, two recent studies have shown that the TLCD damper parameters should be properly optimized for this structure given the complex dynamic conditions of the offshore wind turbine, especially due to the wind turbulence that cannot be equated with sine stimulation and the effects of gust, wind cutting, and turbulence as well as the pitch controlling and the stall dynamic system of the turbine should be considered. In other words, it should be possible to estimate the reduction rate of responses during the presence of the damper with the changes in the main parameters of the damper. Therefore, since it was found in the research that no regular process and definite relationship can be achieved for this issue, in this research, we used the artificial neural networks method to estimate the reduction rate in the response rate of the offshore wind turbine in case of employing the TLCD damper with changes in its main parameters. We used an offshore wind turbine with three different supporting platforms at different depths of the sea instead of a one-degree of freedom structure in this paper to reduce the uncertainties in the optimal parameter relationships. Also, a set of simultaneous combination of wind and wave loads was used to find these parameters. By applying the above, these conditions can be brought into reality as much as possible so that the outputs would be more reliable.

## 2. Governing Equations of OWT with TLCD

Energy absorbers reduce the response of the structure under dynamic loads by absorbing some of the energy input to the structure. The above explanation is based on energy, although it can also be explained based on force. The energy absorbers have a vibrational mass called the secondary mass. The secondary mass applies force to the main structure with its vibration. If the energy absorber frequency is tuned (set), this force acts in a way to reduce the response of the original structure. Simply put, when the main structure moves

to the right, this force enters the main structure in the left direction, and vice versa, when the main structure moves to the left, the power is applied to the right. The above force is the result of two forces: The force resulting from the total inertia of the TLCD due to the absolute acceleration of the structure (the acceleration of a point of the structure where the TLCD is installed) and the force generated by the inertia of fluid movement inside the horizontal column of the TLCD. It should be noted that in the case of the second force, only the motion of the fluid in the horizontal column is raised as the movement of fluid in the vertical columns causes the applied vertical forces, which do not affect the lateral response of the structure. If the first force is represented by  $F_1$  and the second force with  $F_2$ , we would have:

$$F_1 = m_f \ddot{x} \quad , \quad F_2 = \rho B A_b \lambda \ddot{y} = \rho B A_h \ddot{y} \quad (1)$$

It's worth noting that in the above equation, only  $F_2$  reduces the response of the main structure and  $F_1$  actually raises the responses since the force  $F_1$  in the direction of the inertia force of the main structure but the force  $F_2$  is in the opposite direction. However, the values of these two forces are such that their outcome leads to reduced responses. In other words, the absolute value of  $F_2$  is greater than the absolute value of  $F_1$  (in the circumstance that the damper parameters are optimal). With the algebraic summation of the two above-mentioned forces, the force applied by the TLCD to the structure is obtained as follows.

$$F = m_f (\ddot{x} + \bar{k} \ddot{y}) \quad , \quad \bar{k} = \frac{B}{2h + B/\lambda} \quad (2)$$

In the above equation, the fluid weight inside the TLCD is shown with  $m_f$ ,  $x$  also represents the local displacement of the structure where the TLCD is located and the above force is applied at the same point to the main structure. It should be noted that the mass of the TLCD pipes is usually ignored or their mass is considered in the mass of the main structure. Also, the equation of the fluid flow (movement) in the damper, based on which, the acceleration values of the fluid are obtained in the horizontal  $\ddot{x}$  and vertical  $\ddot{y}$  columns to be used in Eq. (2), is described in details in [8].

In the end, the motion equation of the multi-degree system of the offshore wind turbine along with the damper can be written in the form of a matrix as follows.

$$[M]\{\ddot{u}\} + [C]\{\dot{u}\} + [K]\{u\} = [F]_{Aero} + [F]_{Hydro} + [F]_{Tlcd} \quad (3)$$

Wherein:  $[M]$ : Structure mass matrix;  $[C]$ : The structure intrinsic damping matrix considered as such

due to the Cauchy damping factor so that the damping ratio in all modes would be equal to 2%. The complete details of the Cauchy damping method are presented by Chopra (1995) [11].  $[K]$ : Structure hardness matrix;  $\{u\}$ ,  $\{\dot{u}\}$ ,  $\{\ddot{u}\}$ : Vectors of displacement, velocity, and acceleration of the structure response;  $[F]_{Aero}$ : The vector of aerodynamic forces (These forces are calculated by the FAST program [12] and only enter the turbine system section and are equal to zero on the support platform);  $[F]_{Hydro}$ : The vector of hydrodynamic forces (These forces are calculated using the modified Morrison equation [13] only enter the turbine system section and are equal to zero on the support platform);  $[F]_{TlCGD}$ : The vector of the TLCGD force (This force is calculated using equation 2 and only applies to the NACELLE turbine level and is zero at other levels of the system [14])

It should be noted that due to the use of the centralized mass model and considering that the mass of each level is concentrated in only one point, then, the number of degrees of freedom of the system is the same as the number of the levels considered.

### 3. Simulation of the OWT -TLCGD in the Simulink

Simulink is a simulation tool equipped with MATLAB software. Simulink has general applications and is not limited to any particular uses like many other engineering simulation software. Using the Simulink, we can dynamically analyze the behavior of a system without the need to build it and only by having the mathematical relations governing that system by saving time and cost [15]. In the present paper, we used this tool for modeling and analysis due to the large volume of computations as well as the interaction and coupling equation between the structure, and damper, and aerodynamic and hydrodynamic loads.

There are two ways to model damper in the Simulink:

1. Considering the location of the TLCGD as a separate alignment (level); In case of using this method, the matrices of mass, stiffness, and damping of the structure will change in the non-TLCGD state.
2. Applying the corresponding TLCGD force into its location; in case of using this method, the structure and TLCGD can be analyzed with their own specifications separately and without any changes.

In this paper, the second method was used for simulation in the Simulink. To use this method, the multiple-degrees of freedom structure is stimulated by a single stage of loading. Therefore, for an n-degrees of freedom structure, we will have:

$$[M]_{n \times n} \{\ddot{u}\} + [c]_{n \times n} \{\dot{u}\} + [k]_{n \times n} \{u\} = \begin{Bmatrix} F_1 \\ F_2 \\ \vdots \\ F_n \end{Bmatrix}_{n \times 1} \quad (4)$$

Hence, the acceleration at the point of the structure where the TLCGD is placed (usually the highest level of structure) will be obtained. Therefore, the TLCGD is analyzed as a one-degree of freedom system with an absolute acceleration, which is the result of the earthquake acceleration and the acceleration of the level where the TLCGD is placed. The corresponding TLCGD force will be obtained by multiplying the TLCGD mass by its absolute acceleration, which can be applied to the structure at the level where the TLCGD is placed. By applying the force corresponding to the TLCGD to the n-th level of the structure, in Eq. (4), the force term is changed as follows:

$$\begin{Bmatrix} F_1 \\ F_2 \\ \vdots \\ F_n + F_{TLCGD} \end{Bmatrix}_{n \times 1} \quad (5)$$

According to the description and equations presented above, the block designed in the Simulink for a wind turbine equipped with a TLCGD damper is obtained as shown in Fig. 1. It should be noted that the model is analyzed once as shown below to examine the performance of the damper in reducing vibrations for each load combination applied to the system. Once again, the other model is analyzed by cutting off the damper force path in the Simulink to perform a comparison between the mode with and without the damper.

The numerical algorithm which is used in Simulink model, is Runge–Kutta method. In numerical analysis, the Runge–Kutta methods are a family of implicit and explicit iterative methods, which include the well-known routine called the Euler Method, used in temporal discretization for the approximate solutions of ordinary differential equations.

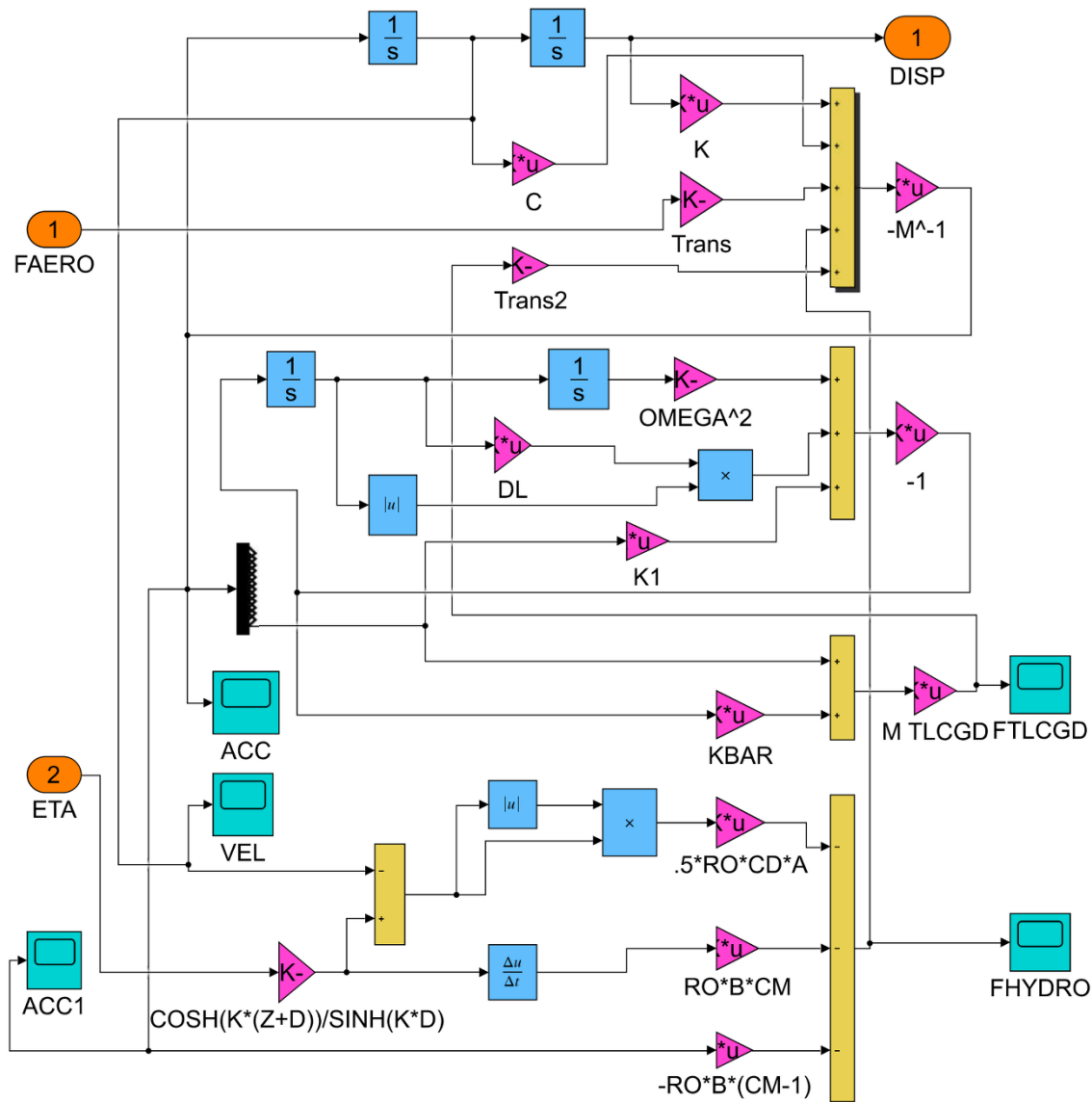


Figure 1. The block designed in the Simulink for an offshore wind turbine equipped with TLCGD

#### 4. Artificial neural network

By observing biological systems and natural systems, the scientists provide some descriptions for them. These mathematical descriptions were then converted into a series of computational blocks. These blocks emerged in the form of neural networks, genetic algorithms, particle swarm algorithms, etc., which are called computational intelligence. The most important feature of these algorithms is to inspire from nature since the nature has chosen almost the best possible solution due to having sufficient time [16].

The artificial neural network, which is a data processing system, has been designed and introduced with inspiring from the human brain in pursuit of faster processing and solving the problems. In the neural networks, data processing is handled by small processors working together in an interconnected and parallel network. The benefits of this artificial network include the high speed and responding as well as the ability to answer unanswered questions based on experience and training. In other words, with more data used to train the neural network, the neural

network will be trained more accurately and will experience less error when producing output [16].

Flood and kartam raised the use of artificial networks in civil engineering for the first time. In their paper, they used the popular form of the supervised progressive neural network. In this article, a graphical interpretation of the neural network was introduced for the first time. In fact, the purpose of this paper was to ensure the development of this technology in the civil engineering [17].

In those years, the artificial neural network was developed in areas such as optimization process, seismic hazard prediction, classification of non-destructive evaluation signals, structural value estimation, etc. In recent years, the use of artificial neural networks and the optimization algorithms have drawn much attention in controlling the vibrations. In this regard, Leung et al. (2008) obtained the optimal TMD frequency and damping ratio for a one-degree of freedom structure under the non-fixed basic vibration using the Particle Swarm Fractional Algorithm (PSO) [18]. In another study in 2009, Leung and Zhang used the PSO algorithm to obtain the optimal parameters

for a one-degree of freedom structure under external loading and basic vibration modeled with the white Gaussian noise and provided formulas for these values [19]. Also, in 2011, Bekdas and Nigdeli used the Harmony Search (HS) algorithm to find optimal TMD parameters for a 10-story structure under the harmonic basic acceleration [20]. Moreover, in 2019 ANN was used for prediction the wave set-up in Iranian coasts [21].

#### 4.1. Neural network data

In this paper, it will be used the modeling and approximation feature of the neural network functions to estimate the reduction percentage of the response of an offshore wind turbine with TLCGD. This system is under different wave and wind excitations. Finally, frequency and mass of the TLCGD are optimized. Three offshore wind turbines simulated in the Simulink were placed under simultaneous stimulations caused by wind and wave. To this end, 75 different loadings of wave and wind applied to the offshore wind turbines were used to optimize these parameters as follows.

**Table 1. Specifications of simultaneous wind and wave loadings**

Parameters	Range
$u_{wind}$ (Average Wind Speed)	$8 \frac{m}{s} \xleftarrow{2 \text{ Spaced}} \rightarrow 24 \frac{m}{s}$
$H_{wave}$ (Significant Wave Height)	$2m \xleftarrow{2 \text{ Spaced}} \rightarrow 10m$
$T_{p_{wave}}$ (Peak Wave Period)	$8s \xleftarrow{4 \text{ Spaced}} \rightarrow 16s$

The optimization index is the reduction rate of the mean SD (standard deviation) of the structure response displacement at the level of damper placement for 75 different loadings compared to the absence of damper case. To increase the number of data for artificial neural network training as well as reducing the uncertainties, three values of 2%, 4%, and 8% were considered for the ratio of the mass of the damper to the mass of the structure ( $\mu$ ) and three values of 0.6, 0.7, and 0.9 for the ratio of the damper frequency to the frequency of the structure ( $\alpha$ ).

The data in the neural network is divided into three categories:

1. Training data
2. Validation data
3. Testing data

A total of 2025 data were used to train the neural network. The information was provided based on the outputs of three offshore wind turbines under 75 combinations of loading, which were obtained for the ratios of different masses and frequencies. Of this information, 70% was the share of training data, 15%

of the validation data, and 15% of the experimental data share.

The neural network takes a part of the data as questions and answers and teaches the neurons accordingly. Then, during the training, it provides the neurons some of the data unanswered to test the training process and uses a portion of the data in the end for the final test, which is not used in the training and validation processes. The similarity of validation data and experimental data is that for both, the data is given to the neurons unanswered. But the major difference between them is that the validation data is used during the training process to prevent data memorizing by neurons, while the test data is used at the end of the training process to evaluate the system's performance. The following parameters were used as inputs to train the neurons:

- The frequency of the first mode of the offshore wind turbine
- The ratio of the TLCGD mass to the structure mass ( $\mu = \frac{m_{tlcgd}}{M_{structure}}$ )
- The ratio of the TLCGD frequency to the structure frequency ( $\alpha = \frac{\omega_{tlcgd}}{\omega_{structure}}$ )

Since the inputs are not of the same type, all the inputs and outputs data were normalized to better assess the performance of the neural network. Also, with trial and error process to get the best answer, finally, three hidden layers were used with each containing 10 neurons and the one output layer was considered. It should be noted that, as shown in Fig. 2, the number of output layers is always equal to the number of outputs of the neural network. The output of the neural network is the percentage of reduction of the structure response in the mode with the damper compared to the mode without the damper. Thus, the user receives the performance rate of the TLCGD in reducing the structure response as output by entering some specifications of the offshore wind turbine and the TLCGD damper installed in it such as the frequency of the structure, the ratio of the damper mass and the ratio of the damper frequency. In other words, this process leads to the optimal design of this damper for a variety of wind turbines with different frequencies. Since if, for example, the percentage of reduction in the structure response, which is the output of the neural network, becomes negative or reduces, it means that the two main parameters of TLCGD, ( $\mu$ ) and ( $\alpha$ ), are not properly selected. It implies that the damper function has been destructive or has not functioned properly.



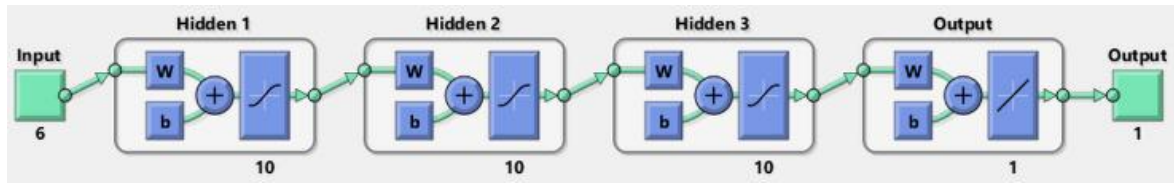


Figure 2. Specifications of the artificial neural network input and output layers

#### 4.2. The results of artificial neural network

Using the artificial neural network, the system could train the neurons well after about 12 iterations. As shown in Fig. 3, aimed at reducing the mean square, the system has well reduced the square errors in the training, validation and testing data.

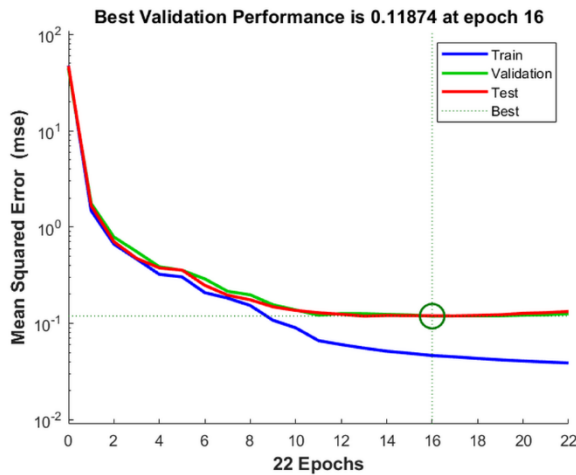


Figure 3. The trial and error process of the neural network for training the neurons

This network is designed in such a way that in the absence of improvement up to six consecutive stages in the neural network training process, the algorithm will stop and the best answer to that stage will be identified. According to Fig. 4, a little improvement is seen in epoch 12 compared to epoch 11; but, after repeat 12, there are three stages of failure to improve compared to step 12. However, at the end of step 16, the system will perform better than the previous steps; and then, the 6 non-improvement steps will stop the training algorithm. Finally, the sixteenth epoch is selected as the best performance. In Fig. 4,  $\mu$  is the control parameter for the algorithm used to train the neural network. Choice of  $\mu$  directly affect the error convergence.

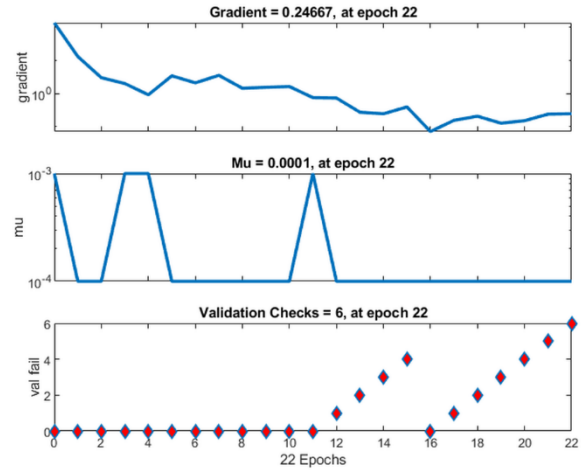


Figure 4. The improvement steps of neural network training

By training the neural network, the target values and the output of the neural network are compared as follows.

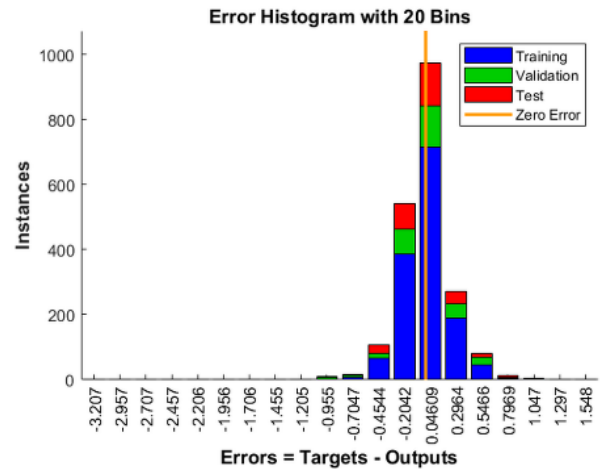


Figure 5. Error Histogram Diagram

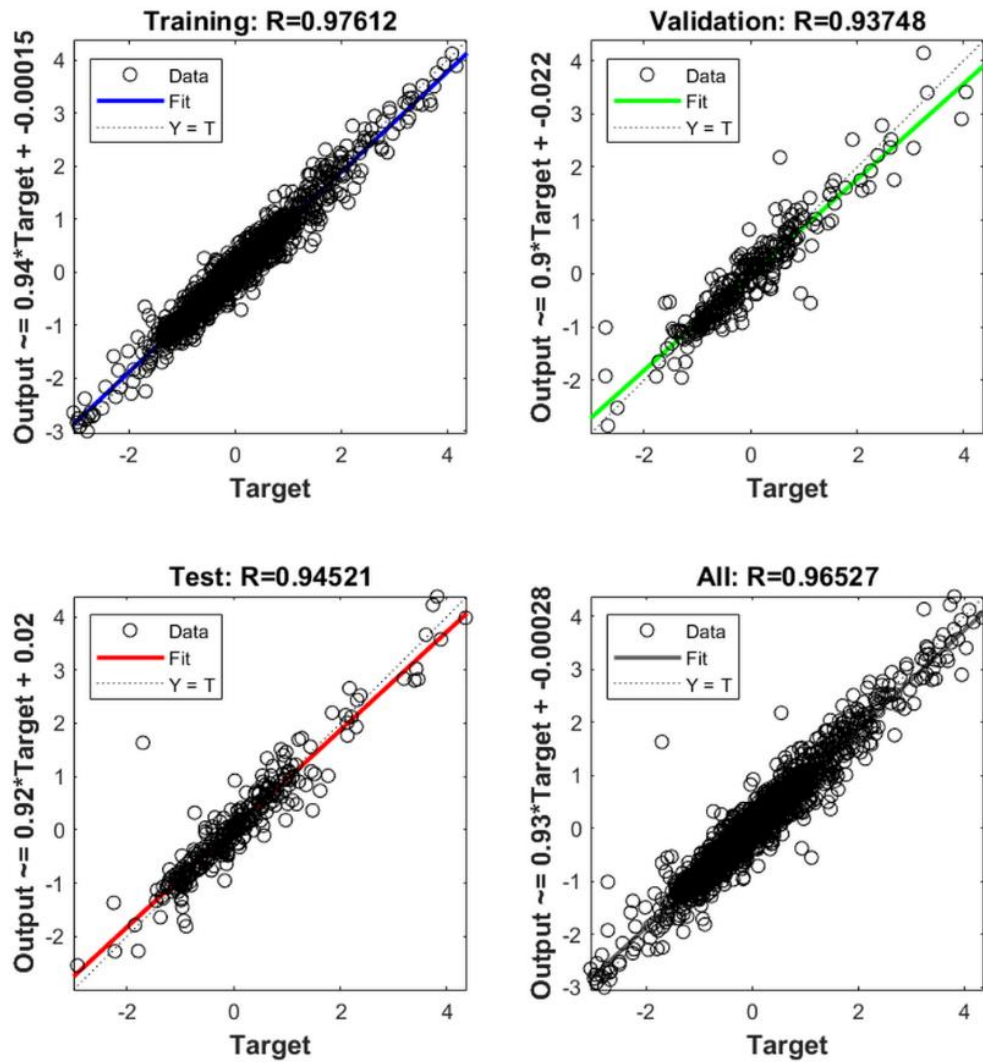


Figure 6. Comparing the correlation between the values of the reduction percentage of the actual response and the values obtained from the neural network

## 5. The use of ANN to optimize TLCGD performance in OWT

In this section, to control the results obtained by the artificial neural network, an offshore wind turbine associated with a TLCGD damper with the characteristics shown in Fig. 7 were put under 75 combinations of load in the previous section; then, the results obtained from Simulink were compared with the results of the neural network. It should be noted that the TLCGD specifications in this section were not used in the neural network training. In other words, the ratio of the mass and the ratio of the current damper are not included in the ratios that were given in the previous section as input to the neural network system. In Fig. 7 the gas is located in the vertical column and on the liquid.

TLCGD is rigidly connected to the primary structure and the relative displacement of the primary structure and the secondary structure is zero. So the stroke which is due to the relative displacement of the TMD to the original structure is not the case in the TLCGD. However, in this damper the similar parameter to the stroke of the TMD, is the displacement of the fluid in the vertical column. Therefore, in this research, the height of the fluid in the vertical column is considered to be 1.5 m before the structural vibration. System analysis under wind and wave excitations showed that the maximum amplitude of displacement of the liquid in the vertical column is about 30 cm. Therefore, in designing the damper, it should be noted that the minimum total height of the vertical column of the damper is about 1.80 meters.

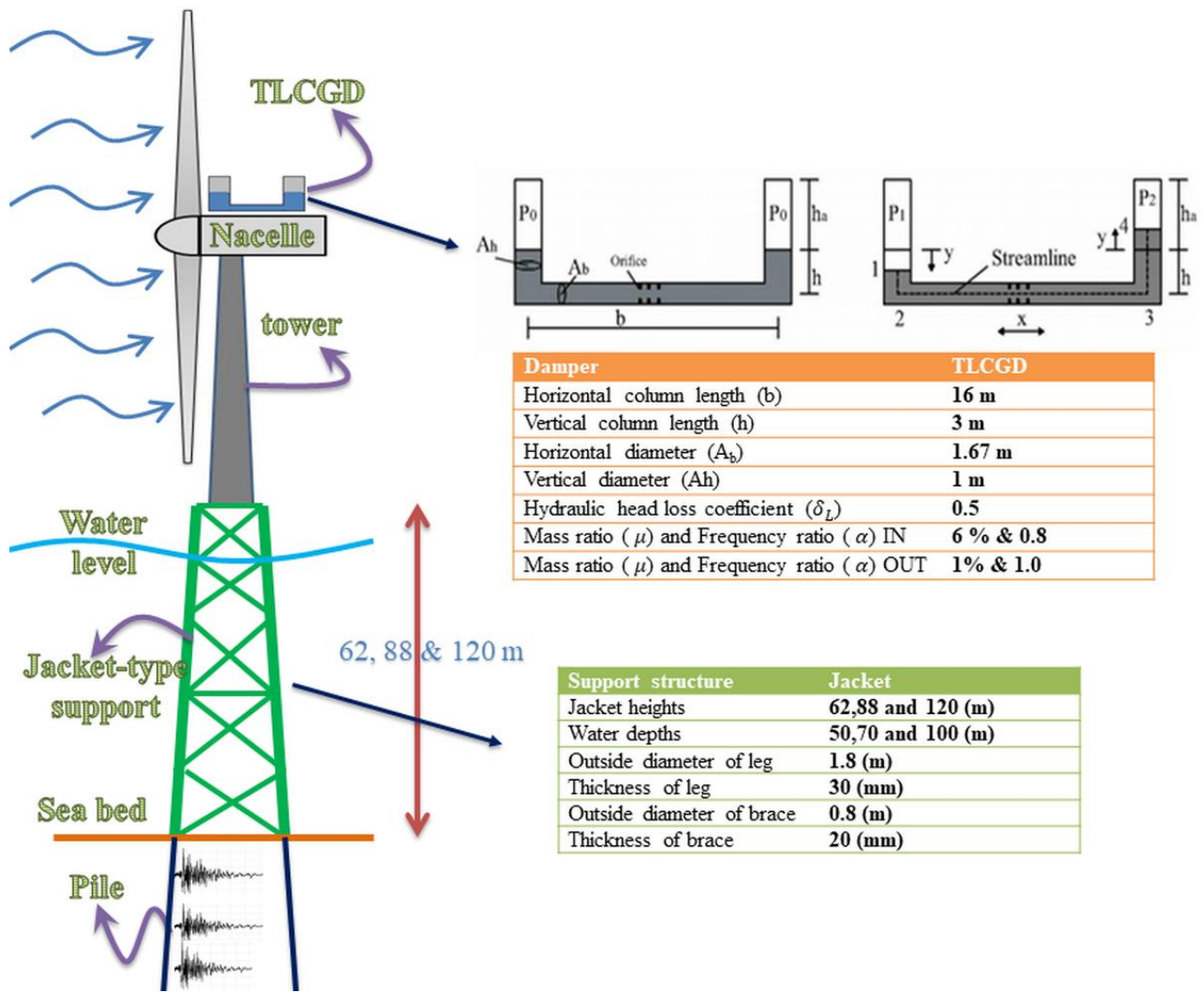


Figure 7. The structure characteristics to control the function of the neural network

As seen in the figure above, new inputs (the damper to structure mass ratio and the damper to structure frequency ratio) have been applied in two different types to examine and control the neural network trained in the previous section. Thus, one of them is within the range of the network training inputs (IN) and the other is outside the range of data used as inputs for training the neural network (OUT). This was done to evaluate the performance of the artificial neural network not only for the known data but also for the data outside the network range and make a comparison between its results and the actual results. To investigate the function of the neural network, the reduction rate in the response of the structure along with the damper obtained from the neural network, which has been under the influence of 75 different

loadings for three different types of turbines (in different depths of water) were compared with the actual results obtained from the Simulink model. In Figure 8, this comparison can be seen for 75 different load combinations.

The structure of the offshore wind turbine is in interaction with the soil that can affect its behavior. This effect increases or decreases in the period of the structure. Therefore, since the purpose of the paper is parametric studies, rather than a case study, different types of OWTs with different periods are considered to evaluation the effects of different types of soil which interaction with structure.



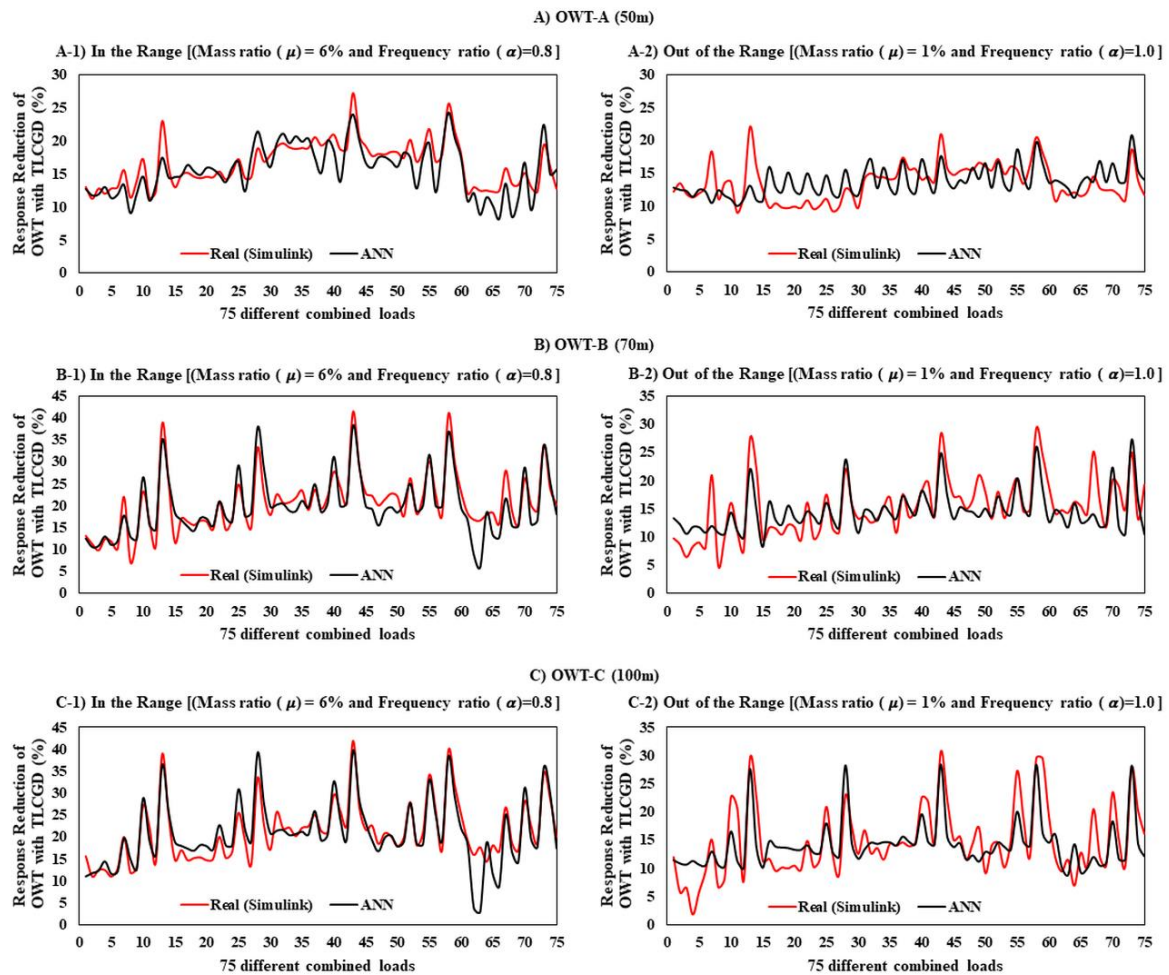


**Figure 8. Comparison of the actual percentage reduction of the structure response with the damper with the percentage obtained from the neural network for 75 load combinations of different simultaneous wind and wave**

Also, for a better understanding, the mean, standard deviation and the effective value (RMS (root mean square)) of Figure 8 diagrams are presented for two types of parameters inside and outside the neural

network training range in Tables 2 and 3 to determine the error percentage of the neural network results compared to the actual results.

**Table 2. Comparison of actual results (Simulink output) and artificial neural network for the state within the training range**

IN [(Mass ratio ( $\mu$ ) = 6% and Frequency ratio ( $\alpha$ )=0.8 ]									
Type of Structure	Mean of response reduction(%)			St. Dev. of response reduction(%)			RMS of response reduction(%)		
	Real (Simulink)	ANN	Error	Real (Simulink)	ANN	Error	Real (Simulink)	ANN	Error
OWT-A (50m)	16.37	15.68	4.21	3.42	3.71	8.57	16.72	16.11	3.65
OWT-B (70m)	20.53	19.95	2.82	6.76	6.77	0.11	21.60	21.06	2.53
OWT-C (100m)	21.07	20.80	1.29	6.81	7.47	9.70	22.13	22.09	0.21

**Table 3. Comparison of actual results (Simulink output) and artificial neural network for the off-range training**

OUT [(Mass ratio ( $\mu$ ) = 1% and Frequency ratio ( $\alpha$ )=1.0 ]									
Type of Structure	Mean of response reduction(%)			St. Dev. of response reduction(%)			RMS of response reduction(%)		
	Real (Simulink)	ANN	Error	Real (Simulink)	ANN	Error	Real (Simulink)	ANN	Error
OWT-A (50m)	13.56	13.73	1.19	2.8702	2.2231	22.55	13.86	13.90	0.30
OWT-B (70m)	15.34	14.52	5.37	5.1519	3.6678	28.81	16.17	14.97	7.45
OWT-C (100m)	14.71	14.24	3.25	6.3003	4.3601	30.80	15.99	14.88	6.94

According to the above tables and Fig. 9, we realize that the proposed neural network has yielded very favorable results for a new input within the range of the training input parameters. Thus, the mean error percentage, the standard deviation and the effective value of the neural network with actual values are below 10% for all three types of the structure. But the results are associated with more errors for a new input outside the range of input parameters of the training of the neural network. However, these error values are still below the 10% in case of average percentage error rate and the effective value; but, the mean percentage error related to the standard deviation is about 20 to 30 percent. The noteworthy point here is that the selected input outside the training range has a damper to structure frequency ratio of 1 associated with the resonance phenomenon. Therefore, one can see that the neural network, despite the fact that it does not know the cause of the phenomena occurred, provides acceptable results even in the presence of an unusual phenomenon.

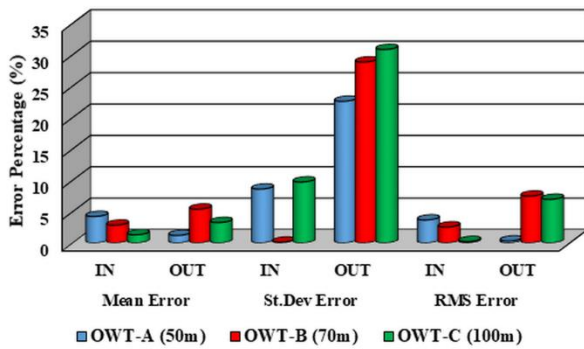


Figure 9. The percentage error rate of the artificial neural network method compared to the actual results obtained from Simulink

## 6. Conclusions

In this paper, we tried to provide a new method based on artificial neural network for examining the optimal TLCGD damper parameters for an offshore wind turbine under the provocations of wave and wind. By considering offshore wind turbines at different depths and combining different simultaneous wind and wave loads, the uncertainties were reduced in obtaining the optimal parameters. As the forces applied to the offshore wind turbine caused by the wave and the wind (especially the wind due to the PITCH control system inside its rotor) have their own intricacies that the regular trend governing the behavior of this type of structure along with the damper cannot easily be determined, the results showed that the neural network was able to somehow detect this behavior and predict the reduction rate of the structure response in the presence of damper according to this model. This will determine the optimal TLCGD parameters for use in different types of offshore wind turbines with different depths and periods. In fact, the importance of using this template is revealed based on the fact that in

defining an analytical or empirical relationship, the impact of some factors has not yet been identified or has been simplified due to the complexity of the behavior. However, by using the neural network, without the need for a complete understanding of the parameters affecting the TLCGD behavior in an offshore wind turbine, these factors are considered indirectly in the prediction of the damper behavior. In this study, to control the accuracy of the neural network performance, two new input categories, including two main parameters of the damper, namely the mass ratio and the frequency ratio, were given to the neural network so that the results can be compared with the actual results of the structure analysis in the Simulink model. These new values were chosen in such a way that, firstly, there will be no recurrent input with the training data of the neural network. Secondly, a bunch of these inputs was outside the range of the neural network training. The results indicated that the neural network has an acceptable error rate compared to the actual results in both categories of inputs. However, this error rate was higher for the category beyond the scope of training, which is normal. Therefore, the method presented in this study can be used practically to determine the optimal parameters of the TLCGD, which will lead to a good design for its use in the offshore wind turbines.

## Acknowledgment

The author acknowledges the funding support of Babol Noshirvani University of Technology through Grant program No. BNUT/394097/98.

## 7. References

- [1] Zhang, P., & Huang, S. (2011). Review of aeroelasticity for wind turbine: current status, research focus and future perspectives. *Frontiers in Energy*, 5(4), 419-434.
- [2] Ogunjuyigbe, A. S. O., Ayodele, T. R., & Bamgboje, O. D. (2017). Optimal placement of wind turbines within a wind farm considering multi-directional wind speed using two-stage genetic algorithm. *Frontiers in Energy*, 1-16.
- [3] IEC, I. (2009). 61400-3, Wind Turbines-Part 3: Design Requirements for Offshore Wind Turbines. *International Electrotechnical Commission, Geneva*.
- [4] Iemura, H., & Pradono, M. H. (2002). Passive and semi- active seismic response control of a cable-stayed bridge. *Journal of Structural Control*, 9(3), 189-204.
- [5] Dezvareh, R. (2019). Upgrading the Seismic Capacity of Pile-Supported Wharfs Using Semi-Active Liquid Column Gas Damper. *Journal of Applied and Computational Mechanics*.
- [6] Lackner, M. A., & Rotea, M. A. (2011). Passive structural control of offshore wind turbines. *Wind energy*, 14(3), 373-388.

- [7] Lackner, M. A., & Rotea, M. A. (2011). Structural control of floating wind turbines. *Mechatronics*, 21(4), 704-719.
- [8] Stewart, G. M., & Lackner, M. A. (2011). The effect of actuator dynamics on active structural control of offshore wind turbines. *Engineering Structures*, 33(5), 1807-1816.
- [9] Dezvareh, R., Bargi, K., & Mousavi, S. A. (2016). Control of wind/wave-induced vibrations of jacket-type offshore wind turbines through tuned liquid column gas dampers. *Structure and Infrastructure Engineering*, 12(3), 312-326.
- [10] Bargi, K., Dezvareh, R., & Mousavi, S. A. (2016). Contribution of tuned liquid column gas dampers to the performance of offshore wind turbines under wind, wave, and seismic excitations. *Earthquake Engineering and Engineering Vibration*, 15(3), 551-561.
- [11] Chopra, A. K., & Chopra, A. K. (1995). *Dynamics of structures: theory and applications to earthquake engineering* (Vol. 2). Englewood Cliffs, NJ: Prentice Hall.
- [12] Jonkman, J. M., & Buhl Jr, M. L. (2005). FAST user's guide. *National Renewable Energy Laboratory, Golden, CO, Technical Report No. NREL/EL-500-38230*.
- [13] Laya, E. J., Connor, J. J., & Sunder, S. S. (1984). Hydrodynamic forces on flexible offshore structures. *Journal of engineering mechanics*, 110(3), 433-448.
- [14] Dezvareh, R. (2019). Evaluation of turbulence on the dynamics of monopile offshore wind turbine under the wave and wind excitations. *Journal of Applied and Computational Mechanics*.
- [15] MATLAB, (2008). *User Guide, Simulink*, MathWorks Inc., Version 7.6.0.
- [16] Haykin, S. (1994). *Neural networks* (Vol. 2). New York: Prentice hall.
- [17] Flood, I., & Kartam, N. (1994). Neural networks in civil engineering. I: Principles and understanding. *Journal of computing in civil engineering*, 8(2), 131-148.
- [18] Leung, A. Y., Zhang, H., Cheng, C. C., & Lee, Y. Y. (2008). Particle swarm optimization of TMD by non-stationary base excitation during earthquake. *Earthquake Engineering & Structural Dynamics*, 37(9), 1223-1246.
- [19] Leung, A. Y. T., & Zhang, H. (2009). Particle swarm optimization of tuned mass dampers. *Engineering Structures*, 31(3), 715-728.
- [20] Bekdaş, G., & Nigdeli, S. M. (2011). Estimating optimum parameters of tuned mass dampers using harmony search. *Engineering Structures*, 33(9), 2716-2723.
- [21] Dezvareh, R. (2019). Providing a new approach for estimation of wave set-up in Iran coasts. *RESEARCH IN MARINE SCIENCES*, 4(1), 438-448.
- [22] Dezvareh, R., Bargi, K., & Moradi, Y. (2012). Assessment of Wave Diffraction behind the Breakwater Using Mild Slope and Boussinesq Theories. *International Journal of Computer Applications in Engineering Sciences*, 2(2).